JOURNAL OF MATERIALS SCIENCE 30 (1995) 2463–2474

Review
The positive temperature coefficient of resistivity in barium titanate

B. HUYBRECHTS, K. ISHIZAKI, M. TAKATA
Nagaoka University of Technology, Kamitomioka 1603-1, Nagaoka, Niigata 940-21, Japan

Positive temperature coefficient of resistivity (PTCR) materials have become very important components, and among these materials barium titanate compounds make up the most important group. When properly processed these compounds show a high PTCR at the Curie temperature (the transition temperature from the ferroelectric tetragonal phase to the paraelectric cube phase). In the first half of this paper literature related to the resistivity-temperature behaviour is discussed. As explained by the well established Heywang model, the PTCR effect is caused by trapped electrons at the grain boundaries. From reviewing experimental results in the literature it is clear that the PTCR effect can not be explained by assuming only one kind of electron trap. It is concluded that as well as barium vacancies, adsorbed oxygen as 3d-elements can act as electron traps. In the second half of this paper, the influence of the processing parameters on the PTCR related properties is discussed. Special emphasis is placed on the phenomenon that the conductivity and grain size decrease abruptly with increasing donor concentration above ~ 0.3 at%. Several models explaining this phenomenon are discussed and apparent discrepancies in experimental data are explained.

1. Introduction

1.1. What are PTC(R) materials ?

Although the acronym PTC, positive temperature coefficient, is a very general term, it has been narrowed to label a very specific phenomenon. The first restriction is that PTC terms an *anomalous* positive temperature coefficient. This is still very broad and also includes the shape-memory alloys which exhibit an anomalous PTC of expansion [1]. This is, however, not what is generally understood by PTC. In fact, PTC is used as an abbreviation of another acronym PTCR, the PTC of resistivity.

In spite of the fact that PTCR is narrower than PTC, it includes the superconductors which have a high PTCR at their critical temperature, T_c. However, the superconductors are not included in the PTCR-family. In fact, the PTCR materials can be divided in four groups: polymer composites, ceramic composites, V_2O_3 compounds and $BaTiO_3$-based compounds ($BaSrTiO_3$, $BaPbTiO_3$, . . .).

The polymer composite PTCR materials are based on a semi-crystalline (polyethylene) or amorphous polymer matrix (epoxy) with a dispersion of conducting particles (carbon, borides, silicides, . . .). When the conducting particles form connecting path-ways, the conductivity at room temperature is high. The PTCR phenomenon is caused by a large volume expansion near the melting point for the semi-crystalline, and at the glass transition point for the amorphous, polymers. When properly made, the particles are disconnected by the volume expansion and the resistivity increases very quickly [2, 3].

These polymer PTCR materials have lower room temperature resistivity and better shock resistance than the $BaTiO_3$-based compounds. There is a large negative temperature coefficient (NTC) effect at high temperatures due to the rearrangement of the conducting particles [3]. Also, electrode cracking due to the volume expansion and thermal deterioration by heat cycles causes problems [3].

The principle for the PTCR in the ceramic composite PTCR materials, is the same as for the polymer PTCR materials. Conducting particles (carbon, antimony-doped SnO_2, . . .) are mixed with a ceramic (SiO_2, ZrP_2O_7, . . .) in order to form conducting pathways. The particles are disconnected by the large volume expansion at phase transformations, which increases the resistivity. The PTCR effect in such a composite has already been reported by Kato *et al.* [4]. Because the observed jump was very small (< 1 order of magnitude) little attention has been paid to this kind of PTCR ceramic. Recently, however, a PTCR effect of three orders has been reported for an antimony-doped SnO_2–SiO_2 composite [5]. The lack of reproducibility due to oxidation and matrix cracking must be overcome before these materials can be useful [5, 6].

The third group are the V_2O_3-based compounds. These compounds exhibit metal insulator (MI) transitions at which they have a sharp PTCR. The transition temperature can be controlled by adding titanium or chromium. This PTCR effect has been considered for practical use [7, 8]. The MI transitions

0022–2461

in these compounds have been studied intensively over the past 40 years. However, a detailed evaluation of the PTCR in these compounds would lead us beyond the scope of this review. For a detailed review concerning the MI transitions, see Yethiraj [9].

The fourth group are the $BaTiO_3$-based compounds. The PTCR effect of $BaTiO_3$ was originally developed in the early fifties in the Philips Research Laboratories in the Netherlands [10]. $BaTiO_3$ which is an insulator at room temperature becomes semiconductive after doping with trivalent donors (e.g. La, Sb, Y) which substitute for the Ba^{2+} or with pentavalent donors (e.g. Sb, Nb, Ta) which substitute for Ti^{4+}. When properly processed, semiconductive $BaTiO_3$ shows a PTCR effect (Fig. 1). The temperature at which the anomaly occurs can be altered by adjusting the Curie point, T_c (the transition temperature of the transformation from the ferroelectric tetragonal phase to the paraelectric cubic phase). The Curie point can be easily changed by doping with strontium or lead, which both substitute for barium. Strontium addition lowers the T_c, while lead increases it [11]. PTCR thermistors with a T_c up to 300 °C are now commercially available [12]. Using lead-doping, several attempts were made to obtain PTC thermistors with even higher T_c [13–16]. This has been shown to be difficult because of lead evaporation during sintering. Recently there have been reports of a PTCR effect at 700 °C in $Ba_{1-x}Sr_xPb_{1+d}O_{3-d}$ ceramics, but the mechanism seems to be different from that for the traditional $BaTiO_3$-based PTCR ceramics [17].

The PTCR effect in $BaTiO_3$-type compounds has been, and still is, a very important research topic, because of its technical importance and the difficulty of explaining the behaviour thoroughly. This paper reports not only the most important developments in the $BaTiO_3$-type PTCR ceramics, but results are reordered and re-discussed in order to explain apparent discrepancies.

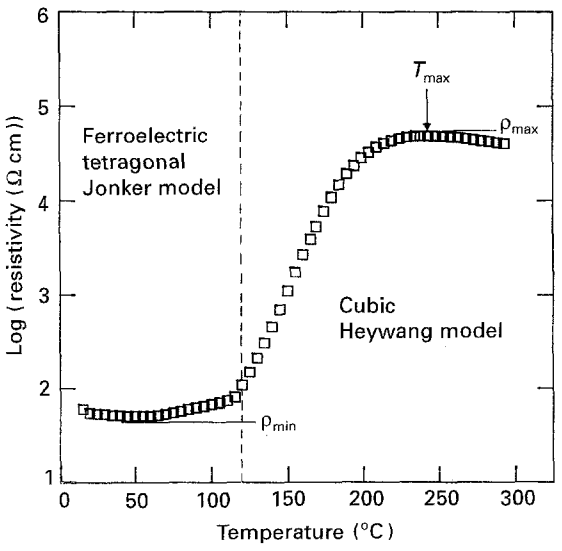

Figure 1 Typical resistivity behaviour of a $BaTiO_3$-type PTCR material.

1.2. Applications

Some typical PTCR components for specific applications are shown in Fig. 2. The applications of $BaTiO_3$-type PTCR ceramics can be classified in three main groups, see Table I. The applications which use the PTCR thermistors to limit the electrical current constitute the first group. This group can be subdivided in two other groups; applications which use the attenuation of the current, and those which use the attenuation rate of the current. The applications using the V–I characteristic for constant temperature heating form the second group. The third group of applications are the temperature sensors which use the R–T characteristic of the ceramic. Examples of each group are given in Table I. Improved quality control and reliability (see Fig. 3) are just two of the factors which have led to a worldwide production of about 450×10^6 pieces/year [18], triple the amount produced in 1980 [19].

2. The temperature–resistivity relation

2.1. The Heywang model

The most accepted model to explain the temperature resistivity behaviour above the Curie point in donor-doped $BaTiO_3$-type is the Heywang model first published in 1961 [20–22]. Heywang assumed a two-dimensional layer of electron traps, also called acceptor states, along the grain boundaries, see Fig. 4. These electron traps attract electrons from the bulk resulting in an electron depletion layer with width, b

$$b = \frac{N_s}{2N_d} \tag{1}$$

where N_s is the density of trapped electrons at the grain boundaries and N_d the charge carrier concentration. This depletion layer results in a grain-boundary barrier, ϕ_0

$$\phi_0 = \frac{eN_s^2(T)}{8\varepsilon_0\varepsilon_{gb}(T)N_d} \tag{2}$$

where e is the electron charge, ε_0 the permittivity in free space and ε_{gb} the relative permittivity of the

Figure 2a

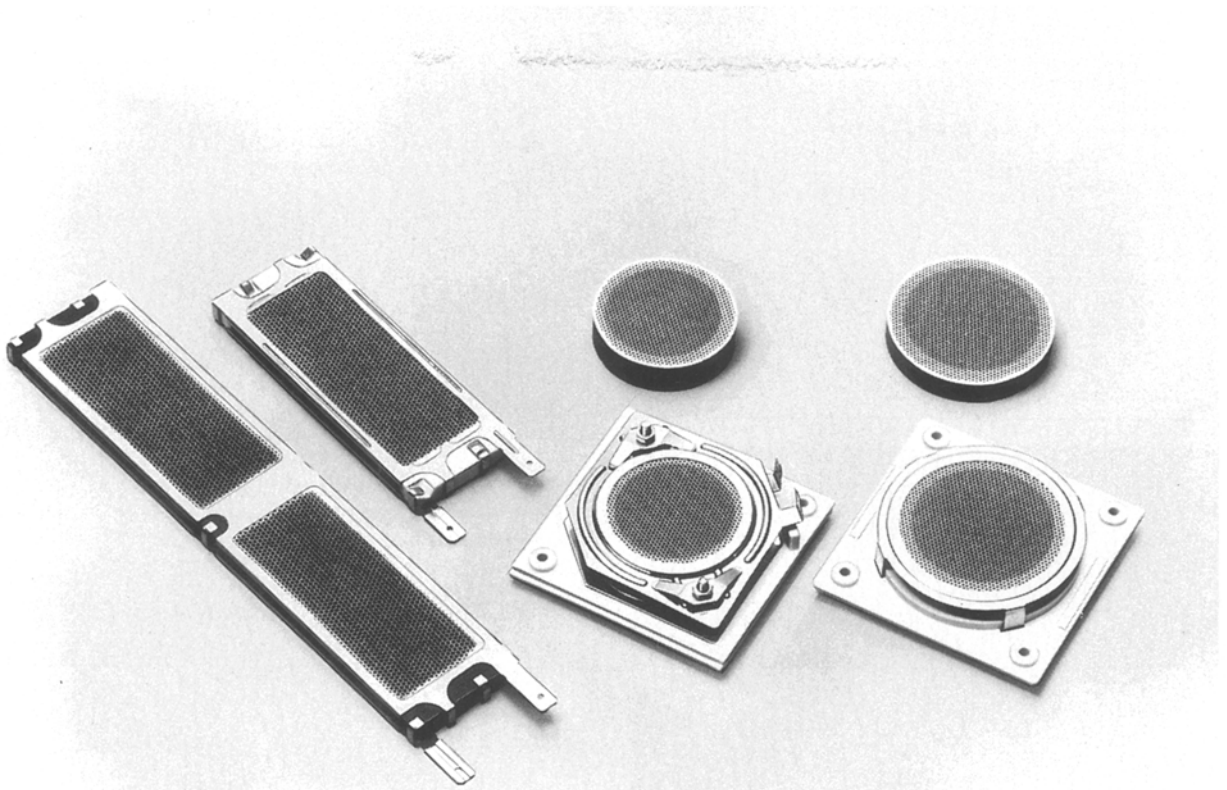

(b)

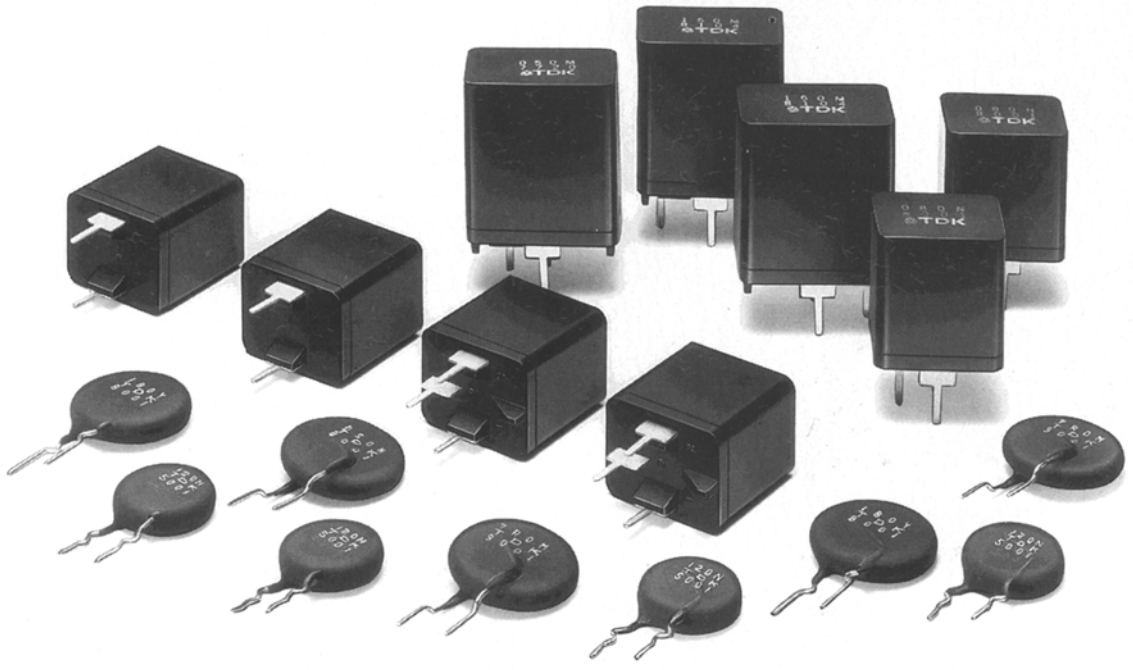

(c)

Figure 2 Some typical PTC thermistors made by TDK. (a) PTCR components for motor starting, (b) honeycomb heaters for drying purposes, and (c) thermistors used in degaussing circuits of colour TVs and monitors.

TABLE I Classification of the PTCR applications

Current limiters
using the attenuation of the current
fuses
using the attenuation rate of the current
colour TV and computer display degaussers
motor starters
Constant temperature heaters
using the I–V characteristic
mosquito killers
hair driers
heaters in trains and cars
Thermal sensors
using the R–T characteristic

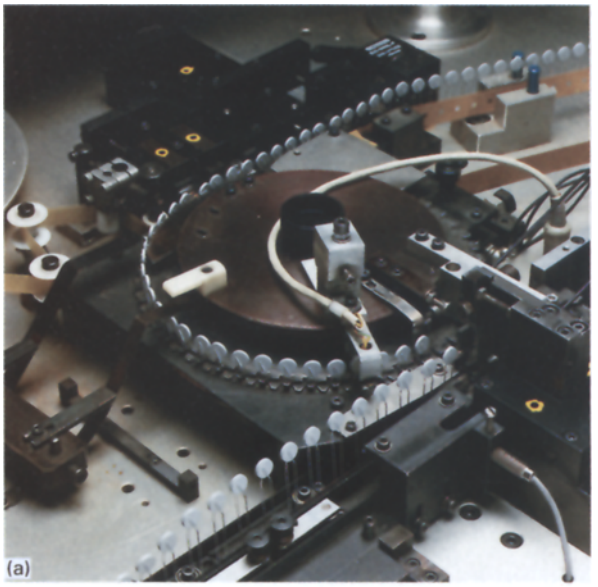

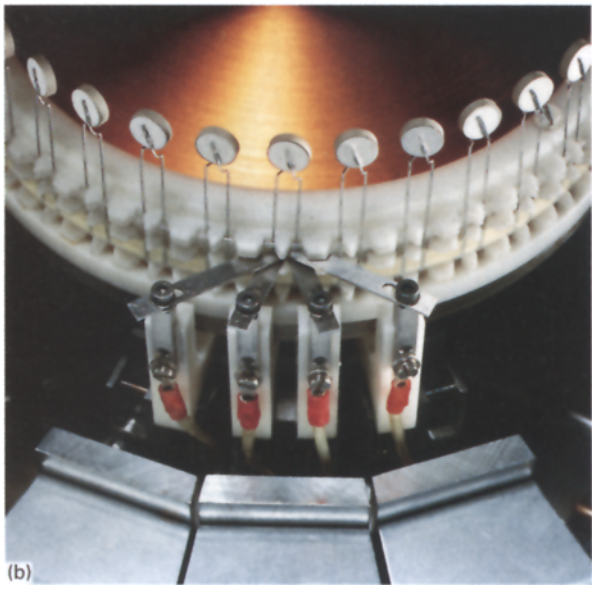

Figure 3 PTCR components are subjected to a vigorous quality testing. (a) The PTC thermistors undergoing a final test before being mounted on top tape (Philips Component Industrial, Brussels). (b) The resistivity at 25 °C is tested in a temperature-controlled environment (Philips Component Industrial, Brussels).

grain-boundary region. The barrier height is also a function of pressure, leading to the piezoresistive effect in semiconductive PTCR ceramics. This

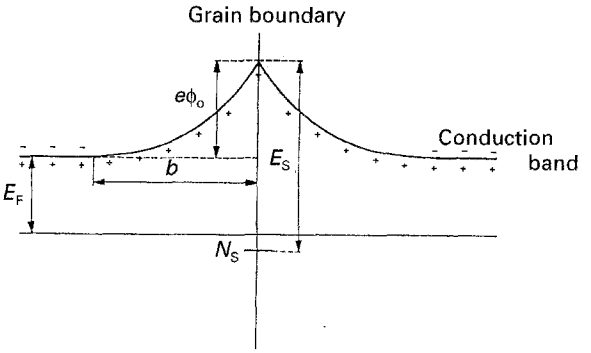

Figure 4 The potential barrier caused by a two-dimensional electron trap along the grain boundaries, where b is the depletion layer width, N_s the density of trapped electrons, E_s the electron-trap energy, $e\phi$ the potential barrier, and E_F the Fermi level (after Jonker, reprinted from [22] with permission from Pergamon Press Ltd, Oxford, UK).

phenomenon is well reviewed by Amin [23], and will not be discussed here.

The resistivity of the sample, ρ, is related to the potential barrier by

$$\rho = A \exp\left(\frac{e\phi_0}{kT}\right) \tag{3}$$

where A is a constant and k the Boltzmann constant. To be exact, A is only slightly dependent on the temperature compared with the exponential term [24].

At the Curie point, the electron traps are well below the Fermi level and the electron trap density, N_{s0}, equals N_s because all electron traps are filled up. Owing to the decreasing grain-boundary permittivity which follows the Curie–Weiss law, the potential, ϕ_0, increases proportionally with temperature. The resistivity increases very quickly as it depends exponentially on the potential barrier, see Equation 3. The electron traps are raised together with the potential barrier and when the energy of the electron traps reaches the Fermi level, trapped electrons start to jump to the conduction band, depressing the increase in ϕ_0 and ρ, and ultimately enhancing the conductivity.

An increase in the energy gap between the conduction band and the electron trap energy, E_s, causes a rise in ρ_{max}, because the energy gap between the electron traps and the Fermi level is bigger. The temperature at which the electrons have enough energy to jump to the conduction band is therefore higher, consequently ρ_{max} and T_{max} are increased by an increase in E_s.

Slightly above the Curie point, T_c, the potential barrier is higher when N_{s0} is higher. When E_s is fixed, the energy gap between the Fermi level and the electron-trap energy decreases with increasing N_{s0}. This means that with rising temperature the electron traps reach the Fermi level at a lower temperature, which leads to a decrease in T_{max}.

In his model, Heywang made three assumptions. First, the PTCR is a grain-boundary effect. Secondly, the grain-boundary permittivity follows the Curie–Weiss law and equals the permittivity of a single crystal. Thirdly, the electron-trap layer is two dimensional along the grain boundaries.

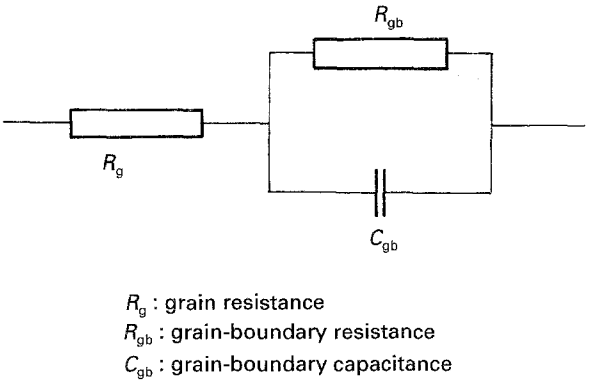

Figure 5 Equivalent circuit for $BaTiO_3$-type PTCR material, as first proposed by Heywang [20].

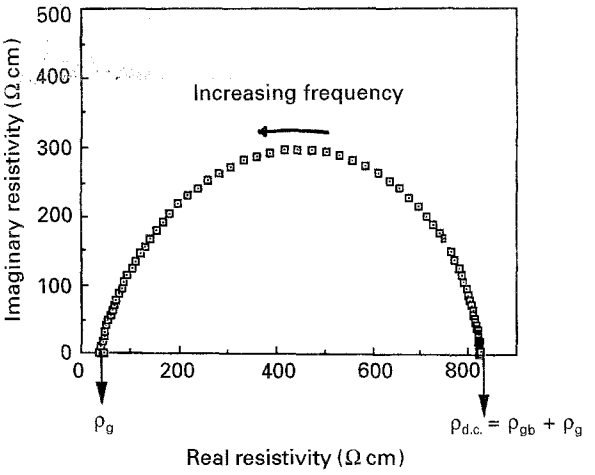

Figure 6 Impedance plane at room temperature for a typical barium titanate PTCR sample. $\rho_{d.c.}$ is the direct current resistivity, ρ_{gb} to the grain-boundary resistivity, and ρ_g the grain resistivity.

$BaTiO_3$ single crystals do not show a PTCR, as was reported by Goodman in 1963 [25]. Grains in polycrystalline ceramics show a negative temperature coefficient (NTC) [26, 27], but a single grain boundary shows a PTCR [26, 27]. These results justify the equivalent circuit for $BaTiO_3$-type PTCR materials in Fig. 5 first proposed by Heywang [20]. Knowing the equivalent circuit, one can easily separate the grain-boundary resistance and the grain resistance using impedance-plane analysis.

The impedance of the RC-parallel combination is given by

$$Z = R_{grain} + [1/(1/R_{gb} + j\omega C_{gb})] \quad (4)$$

where R_g is the intra-grain resistance and R_{gb} is the grain-boundary resistance. The d.c. impedance equals $(R_g + R_{gb})$, while the intercept of the impedance curve at high frequencies with the real axis equals R_g. An example of the impedance plane of a typical $BaTiO_3$-type PTCR material, is given in Fig. 6. Because the depletion layer is much smaller than the grain size, one can easily calculate the grain resistivity using the sample's dimensions.

Impedance-plane analysis for $BaTiO_3$-type PTCR material has been conveniently used for the first time by Maiti *et al.* in 1986 [28] and was later used by many authors [15, 16, 27, 29–32] to separate the grain and grain-boundary resistance.

Recently, Sinclair and West [33] showed that modulus plots of PTCR barium titanate ceramics can provide additional information that cannot be derived from the impedance plane. Combining impedance and modulus plots, they found that there are two components giving rise to the PTCR effects [33], and not just one as assumed before. More work, however, is necessary to characterize the a.c.-response of barium titanate PTCR ceramics, and to propose new or refined models for the PTCR behaviour.

Kuwabara [34] and Illingsworth *et al.* [29] verified that the resistivity–temperature behaviour could be modelled by the equations proposed by Heywang [20–22]. Both found that the equations proposed by Heywang satisfactorily modelled the resistivity behaviour. Illingsworth *et al.* also showed that ϕ_0 is proportional to $(T\text{-}\theta)$ where θ is the Curie temperature. This demonstrated that ε_{gb} obeys the Curie–Weiss law [29], and recently Wang and Umeya reported that ε_{gb} is comparable to the relative permittivity of a single crystal [24]. However, recently it was found that the Heywang model was not able to explain the R–T behaviour very accurately. Better results are obtained by assuming a distribution of the electron-trap energy [35–40].

2.2. The Jonker model

The Jonker model [22], which describes the resistivity below T_c, is a refinement of the Heywang model. Jonker's model is based upon the ferroelectric behaviour of $BaTiO_3$ below T_c. Below T_c, $BaTiO_3$ is ferroelectric with its polarization along the tetragonal crystal axis.

As adjacent grains have different crystal orientations, the polarization direction is different from grain to grain, see Fig. 7. This difference in polarization direction causes a net polarization perpendicular to the grain boundaries, creating surface charges at the grain boundaries. In the case of negative surface charges, which is the case in roughly 50% of the grain-boundary area, the depletion layer is completely or partially filled up. Consequently, the potential barrier diminishes or disappears in height. Half of the grain-boundary area is positively charged, which creates an even bigger potential. However, this does not matter as the conducting electrons always follow the path with the lowest barrier. The spontaneous polarization, P_s, for $BaTiO_3$ is about 0.25 $C\,m^{-2}$ [11]; this is equivalent to 1.6×10^{18} electrons m^{-2}, which is the order of magnitude of N_s in PTCR-$BaTiO_3$. Haanstra and Ihrig showed by TEM studies that a compensation mechanism by local charge compensation is indeed plausible [41]. Recently, Huybrechts *et al.* [42] verified experimentally that there is a compensation mechanism below T_c.

3. The character of the electron traps

3.1. Barium vacancies

The fact that the electron traps form a "two-dimensional" plane along the grain boundaries, as assumed

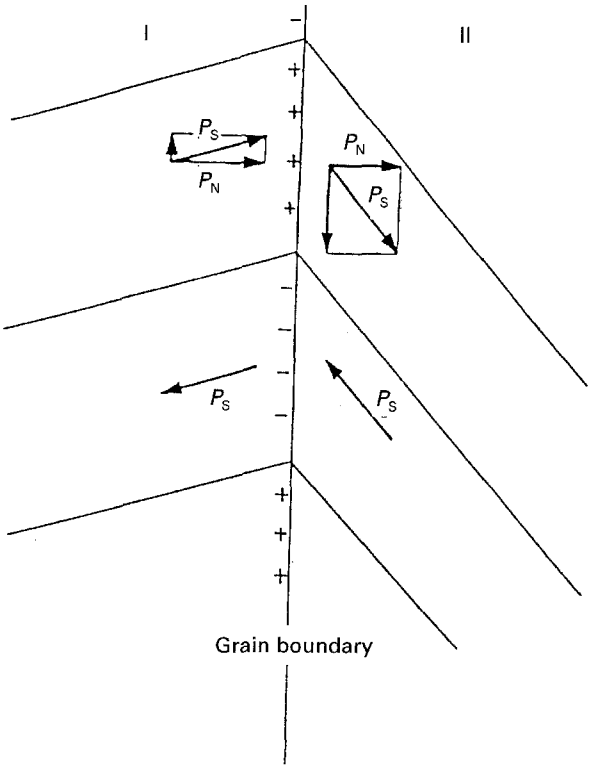

Figure 7 Schematic representation of the ferroelectric domains at the grain boundaries. Owing to the difference of orientation between adjacent grains I and II, a surface charge is produced at the grain boundaries (after Jonker, reprinted from [22] with permission from Elsevier Science Ltd, The Boulevard, Langford Lane, Kidlington OXS 19B, UK.

by Heywang, is disputed by Daniels *et al.* [43]. After studying the thermodynamic equilibrium at high temperature and the kinetic processes during cooling, Daniels *et al.* concluded that the PTCR effect is caused by the defect distribution in the samples and proposed the following mechanism [43]: during sintering, $BaTiO_3$ tends to remain in equilibrium with the surrounding atmosphere. During cooling, the equilibrium barium vacancy concentration $[V''_{Ba}]$ increases, therefore the overall $[V''_{Ba}]$ increases. The V''_{Ba} are produced at the grain boundaries and diffuse from the grain boundaries into the grains. Because the diffusion slows down, the V''_{Ba}-rich diffusion front comes to a standstill. This results in a sample with a conductive grain and an insulating V''_{Ba}-rich grain-boundary zone, as the V''_{Ba} compensate the donors. The V''_{Ba} act as electron traps thereby generating the potential barrier at the grain boundaries.

3.2. Adsorbed gases as electron traps

Several attempts have been made to prove that adsorbed gases play the role of electron traps, as believed earlier [22].

Jonker was one of the first to make such an attempt [44]. Jonker annealed donor-doped $BaTiO_3$ in vacuum and nitrogen. In this way he produced samples without a PTCR jump near the Curie point. After annealing in oxygen or halogen gases at temperatures between 800 and 1000 °C, PTCR jumps of 3–5 orders are obtained. Fluorine, chlorine and bromium annealing was very effective to create electron traps and the accompanying PTCR jump, but iodine annealing had no influence. It was also found that the E_s after annealing in halogen gases such as fluorine, chlorine and bromine was higher than for the oxygen-annealed samples [44]. Although one might expect an influence of the electro-negativity on E_s, there was no big difference between the three different gases, fluorine, chlorine and bromine. Jonker attributes this to a possible deviation from the two-dimensional electron-trap surface-layer, due to diffusion of the halogen atoms into the grains.

Daniels and Wernicke stated that the diffusion of the V''_{Ba} from the grain boundary into the grain is slow and that the diffusion below 800 °C can be neglected [45]. Therefore, attempts have been made to change the PTCR behaviour at low temperatures in short times, in order not to influence the V_{Ba} distribution.

The results of Igarashi *et al.* show that the PTCR jump of a rare-earth-doped $BaTiO_3$ PTCR sample decreased several orders (2–3 orders) when annealed in vacuum (10^{-5} torr; 1 torr = 133.322 Pa). Even vacuum annealing at 300 °C for 1 h decreased the PTCR jump with about 3 orders [46].

Kuwabara produced barium titanate and barium strontium titanate samples with a porosity ranging from 20%–30%, and a grain size of 2–5 μm. Resistivity measurements between room temperature and 400 °C in different atmospheres showed that the atmosphere during measurement had a big influence on the PTCR behaviour. Reducing atmospheres such as nitrogen, CO_2 and CH_4 reduced the PTCR jump slightly, about 0.5–1 order, which is explained by a decrease in adsorbed oxygen.

The PTCR jump was, however, reduced remarkably (more than 6 orders) if measured in CO gas. This can be attributed to oxygen desorption at the grain boundaries or to an increase in charge-carrier density, as CO is known to provide surface donor states in n-type semiconductors [34]. Increasing the charge-carrier density decreases the depletion-layer width, as is shown by Equation 1, and consequently the PTCR jump decreases.

It is shown above that the PTCR behaviour can be changed in a very short time by heat treatments at temperatures too low to change the V''_{Ba} distribution. Therefore, V''_{Ba} are not the only possible electron traps. Further proof is given by the fact that one can obtain a PTCR effect in oxygen-deficient $BaTiO_{3-x}$, which does not contain any V_{Ba}. Alles *et al.* obtained a PTCR in undoped atmospherically reduced $BaTiO_3$ by annealing in fluorine-rich atmosphere. After this treatment, PTCR jumps of 4–5 orders are obtained. The grain resistivity did not change due to the fluorination, which proves that only the grain boundary is influenced by the fluorine-treatment [32]. Takahashi *et al.* repeated a similar experiment. Reduced undoped-$BaTiO_3$ was annealed in air and PTCR jumps up to 5–6 orders were obtained. Electron spin resonance (ESR) measurements showed that adsorbed oxygen was present in the form O_2^- [47]. Because $BaTiO_{3-x}$ does not contain any metal vacancies, only oxygen vacancies, the results of Alles *et al.* [32] and Takahashi *et al.* [47] are very important.

Although it is clear that V''_{Ba} cannot be responsible for the PTCR effect in $BaTiO_{3-x}$, the question still remains if V''_{Ba} act as electron traps in donor-doped $BaTiO_3$. A criticism of the Daniels and Wernicke model is related to the V''_{Ba} diffusion coefficient reported by Wernicke [48]

$$D_{V_{Ba}} = 6.8 \times 10^{-2} \exp\left(\frac{-2.76\,\text{eV}}{kT}\right) \quad (5)$$

With normal cooling rates (1–30 °C min^{-1}) this leads to a grain-boundary zone (GBZ) of 1–3 μm [45]. This means that annealing at high temperatures should lead to further grain-boundary oxidation which finally results in insulating samples. Wernicke reported that fine-grained (2 μm) samples were completely oxidized in only 2 h annealing at 1100 °C in air. Coarse-grained (100 μm) could not be oxidized, even after oxidizing for several days at 1100 °C in air. Although these results are in accordance with the diffusion constant in Equation 5, other researchers' results [49–51] are not. Al-Allak *et al.* annealed non-acceptor-doped samples with a grain size of less than 10 μm up to 27 h at 1220 °C in air. But even after these long annealing times the grain resistivity is not changed and the samples are still semiconductive [49]. If the diffusion coefficient (Equation 5) is reliable, the samples should be completely insulating in less than 5 h. Also Tsai-fa Lin *et al.* could not explain their results by the diffusion coefficient published above [50]. To explain their results Tsai-fa Lin *et al.* proposed the following [50]: at high temperature, V''_{Ba} and $V_O^{\cdot\cdot}$ are generated simultaneously. During cooling, $V_O^{\cdot\cdot}$ diffuse outward, but V''_{Ba} are almost frozen due to their slow diffusion. Therefore, a region with excess V''_{Ba} or a deficit of $V_O^{\cdot\cdot}$ is formed at the grain boundaries. The outward diffusion of $V_O^{\cdot\cdot}$ is, however, slowed down by the formation of $V_O^{\cdot\cdot}$–V''_{Ba} defect complexes.

Recently, it was suggested that the inversion temperature, i.e. the temperature at which V''_{Ba} compensate all donors, depends on the donor-dopant concentration [52]. As this inversion temperature influences the thickness of the grain-boundary zone (GBZ) [52], it might explain the discrepancies discussed above.

Some authors contest the compensation of donors by V''_{Ba}, Lewis *et al.* [53, 54] based on defect-energy calculations and others based on phase studies [55]. However, using cathode luminescence (CL), Koschek *et al.* visualized a GBZ in PTCR-$BaTiO_3$ [56, 57] and the thickness of the GBZ depended on the cooling rate after sintering [56]. These results were explained by an extra energy level in the energy gap, corresponding to the energy level of double-ionized barium vacancies [56, 57].

From the above discussions we can conclude that V''_{Ba} are not the only electron traps. Adsorbed gases can also act as electron traps.

3.3. 3d-elements

It was found by many authors that small additions (0.01–0.1 at %) of some 3d-elements can alter the PTCR behaviour significantly [58–60]. Daniels and Wernicke explained this phenomenon as follows: doping with acceptors with an energy level similar to or higher than that of the electron traps of V''_{Ba} leads to thicker V''_{Ba}-rich GBZ. However, they do not explain why different electron trap energies, E_s, are found, when $BaTiO_3$ is doped with different 3d-elements [45]. Also the electron-trap energy found for acceptor-doped and non-acceptor-doped PTCR materials is different [40, 58, 61]. Therefore, the explanation given by Daniels and Wernicke is at least incomplete. After scanning the 3d-elements, manganese was found to have the deepest trap, thereby giving superior PTCR behaviour [58–60]. Ueoka explained the influence of 3d-element doping as follows [60]: during sintering the extra charge caused by incorporating a metal Mn^{2+} at the Ti^{4+} places is compensated by $V_O^{\cdot\cdot}$, a fact which is proven for non-donor-doped $BaTiO_3$ doped with 3d-elements [62, 63]. During cooling, the grain boundary oxidizes and the $V_O^{\cdot\cdot}$ concentration, $[V_O^{\cdot\cdot}]$, decreases. When the $[V_O^{\cdot\cdot}]$ decreases, the oxidation state of the manganese increases to 3^+ or 4^+ to maintain electroneutrality. The higher oxidation states of manganese act as electron traps and therefore N_s increases during cooling. Although Ueoka proposed this model only for manganese, it can be easily extrapolated to other 3d-elements.

In conclusion, one can say that the results until now cannot be explained by just one kind of electron trap. Therefore, it is believed that as well, V_{Ba} absorbed oxygen as 3d-elements can act as electron traps.

3.4. Other theories

Besides the Heywang model modified by Jonker, several authors have proposed alternative theories. Kutty *et al.* proposed that the PTCR phenomenon is related to a decrease in charge carrier density at T_c [64–66]. Their theory is based on electron paramagnetic resonance measurements. At T_c the activation of V_{Ba} to V'_{Ba} results in a decrease in charge carrier density [65]. Based on the absence of the EPR signal of V'_{Ba} in single crystals, they claim that V'_{Ba} are situated at the grain boundaries. For Mn–La co-doped $BaTiO_3$ they found that manganese is present as Mn^{3+} below T_c, but as Mn^{2+} above T_c. Therefore, manganese acts as an electron trap above T_c, decreasing N_d and consequently enhancing the PTCR effect. Kutty *et al.* claim that for the small manganese concentrations (< 0.1 at %) they studied, manganese is in the bulk crystals and not segregated at the grain boundaries [64].

It is, however, not clear why the manganese, whose concentration is more than ten times smaller than the donor concentration, can influence the charge-carrier density sufficiently to explain the significant increase (several others of magnitude) in PTCR jump by manganese doping.

Based on calculations of bulk and surface defect energies, Lewis *et al.* [53, 54] proposed another theory to model the PTCR behaviour. They found that donor impurities have a lower energy in the bulk. For acceptor states in low-charge states there is a strong tendency for segregation, but for the higher oxidation

states there is no large difference between the bulk and the surface energies. Also, the activation energy for the migration of acceptors in the titanium-sublattice is very high. Therefore, donors will deplete the grain-boundary area, leaving behind an acceptor-rich layer. This leads to n–i–n junctions responsible for the PTCR effect [53, 54]. However, according to more recent segregation studies of Chiang *et al.*, the spacial distribution of the acceptor defects at the grain boundary can be neglected compared to the electron depletion layer width b, see Equation 1. Therefore the acceptor layer caused by segregation can still be assumed as one-dimensional in the Heywang model [67].

Desu and Payne also proposed n–i–n model [68]. They found, contrary to the calculations of Lewis *et al.* [53, 54], that donors segregated to the grain boundaries. If the donor concentration at the grain boundaries exceeds a critical level, the compensation shifts from electron compensation to vacancy compensation. It creates thereby an insulating layer at the grain boundaries [68]. This model is inspired by their explanation of the anomaly of conductivity and grain size. However, that explanation is incomplete as explained in the next section.

4. How do processing parameters influence the PTCR ?

The PTCR behaviour is influenced by many parameters, such as composition, sintering atmosphere, heating rate, cooling rate, and so on. Their interactions and relation to N_{s0}, N_d and E_s, are explained below.

4.1. The anomaly of conductivity and grain size

Very often Al_2O_3, SiO_2 and TiO_2 (AST), are added to $BaTiO_3$ to obtain aeutectic with a low melting point and improve sintering [69–71]. O'Bryan and Thomson reported a eutectic temperature for $BaTiO_3$–$Ba_6Ti_{17}O_{40}$ at 1312 °C [72]. More recent work of Kirby and Wechsler reported an eutectic temperature of 1332 °C [73]. They attributed this big difference to the use of starting materials with high purity. The eutectic temperature is lowered to 1260 °C by adding SiO_2 [74], and is further decreased to about 1240 °C by adding Al_2O_3 [75]. When the eutectic point of the liquid phase is reached, recrystallization occurs in $BaTiO_3$ [71, 75–79]. During the liquid-phase sintering, small grains dissolve in the liquid phase and precipitate at nuclei which grow bigger [76, 79]. Because the recrystallization might result in a few big grains, it is sometimes referred to as abnormal grain growth. This does not suggest that one cannot obtain a homogeneous microstructure by recrystallization. With increasing temperature the nucleation rate increases very quickly [76, 79] which results in a smaller grain size. Well above the eutectic temperature the recrystallization is very fast and the microstructure can be determined in just a few minutes [80]. Therefore, it is possible that the microstructure is formed during the heating process and that the holding time or sintering temperature have no or little influence on the microstructure as is found by several researchers [77, 78, 81]. After the abnormally growing grains have bumped into each other, normal grain growth is very slow [77]. Also, annealing at about 1200 °C for very long times, does not change the grain size significantly [49, 50, 61, 83]. It should be noted that on annealing for several hours below the eutectic point, abnormal grain growth takes place by solid-state transport mechanisms, e.g. surface diffusion in a dense matrix [83].

Recrystallization in $BaTiO_3$ does not take place if large concentrations of donor dopants are added, independent of the kind of dopant. This behaviour is called an anomaly in grain size [30, 84] and it is accompanied by an anomalous decrease in conductivity [14, 21, 22, 30, 85], see Fig. 8. The anomaly of conductivity and grain size occurs at about 0.3–0.5 at % for sintering in air although processing parameters can influence this concentration as is explained below. The anomaly of conductivity is not caused by limited solubility of the donor in the $BaTiO_3$, because it has been shown that the solubility limits for donor dopants are much higher [86, 87] than the concentration at which the anomaly of conductivity occurs.

The anomaly of conductivity is explained by the Daniels *et al.* model as follows. It is known that high dopant concentrations lead to small grain sizes of a few micrometres in general. At practical cooling rates the insulating grain-boundary zone is about 1–3 μm thick. Therefore, small-grained materials become insulators at normal cooling rates [43].

The explanation given by Daniels *et al.* looks very plausible at first sight. However, it does not explain why the grain size changes with increasing amount of dopant (anomaly of grain size). The Drofenik model, on the other hand, relates the anomaly of grain size with the anomaly of conductivity. Drofenik *et al.* found using thermogravimetric analysis (TGA) and

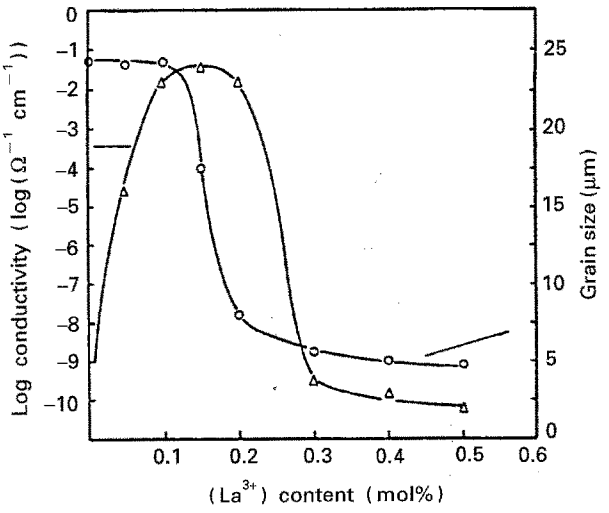

Figure 8 Effect of donor doping on the room-temperature behaviour and grain size of $BaTiO_3$. Notice that the drop in grain size takes place at the same concentration as the drop in conductivity. These phenomena are usually referred to as the anomaly of conductivity and grain size. After Peng *et al.* [30] with permission of the American Ceramic Society.

mass spectrometry that during the crystallization above the eutectic point of the liquid phase, an amount of oxygen proportional to the amount of dopant is released in about 10 min [88, 89]. The reaction which takes place can be written as

$$\text{Oxidized form} \rightarrow \text{reduced form} + O_2 \quad (6)$$

It does not matter if the donor dopant atoms are already incorporated in the $BaTiO_3$ or if the dopant is spread along the surface of the $BaTiO_3$ powder. The weight loss and the oxygen release are the same in both cases [89]. This is in accordance with the model of Hennings *et al.*, because small $BaTiO_3$ grains dissolve in the liquid phase and precipitation of $BaTiO_3$ occurs at bigger grains [76, 79]. Therefore, it makes no difference if the dopant is already incorporated or not. Drofenik *et al.* also found that the maximal amount of dopant which can be added without inhibiting recrystallization, further referred to as the critical donor concentration, depends greatly on the oxygen partial pressure, as shown in Fig. 9 [90, 91]. For the samples with a dopant concentration above the critical dopant concentration, there is no release of oxygen and no grain growth [90, 91].

Drofenik *et al.* explained these results with a thermodynamic model [90]. The formation of the reduced form and the release of oxygen is a non-equilibrium process. Therefore, extra energy should be supplied so that the reduced form can be formed and grain growth can occur. The Gibbs energy for the reaction is given by

$$\Delta G = \Delta G_s + \Delta G_{ss} + \Delta G_{ox} \quad (7)$$

where ΔG_s is the change in Gibbs surface energy, ΔG_{ss} the Gibbs energy of solid solution of dopant in $BaTiO_3$, and ΔG_{ox} the Gibbs energy related to the oxygen release. ΔG_{ss} is very small and can be neglected. ΔG_s is negative, ΔG_{ox} is positive and proportional to the dopant concentration. When ΔG is positive, due to a high dopant concentration, grain growth is inhibited. Using Equation 7, it is possible to calculate the critical donor concentration above which the grain growth is inhibited, as a function of the oxygen partial pressure. The calculated boundary can be expressed in the form

$$\log P_{O_2} = \frac{A}{C_{donor}} - B \quad (8)$$

where A, and B are constants, and C_{donor} is the donor concentration. The calculated boundary agrees very well with the experimental results, proving that the grain size and conductivity anomaly are thermodynamically related [90]. The boundary line drawn in Fig. 9, shows schematically the calculated boundary [90]. As ΔG_s depends on the initial surface energy of the powder, the dopant concentration above which no critical grain growth occurs should depend on the initial surface area of the powder. Drofenik *et al.* confirmed this in [91]. Moreover, when oxygen release is avoided by simultaneous incorporation of another ion compensating the donor ions (e.g. K^+ and Sb^{3+} on barium sites), the grain growth is independent of the donor dopant concentration [92].

A similar compensation mechanism is found when $BaTiO_3$ is donor and acceptor co-doped. It is found that for the 3^+ donor lanthanum and 2^+ acceptors manganese and magnesium (M), recrystallization only occurs when $[La^{3+}] - 2[M^{2+}] < 0.15$. Only the donor concentration remaining after compensation, i.e. $[La^{3+}] - 2[M^{2+}]$, contributes to the semiconductivity [30, 84].

Contrary to Drofenik *et al.*, Al-Allak *et al.* reported that the anomaly of conductivity is not a bulk phenomenon but a grain-boundary phenomenon [51, 93]. Al-Allak *et al.* obtained conductive grains after sintering in air even for holmium donor dopant concentrations up to 1.8 at % [93]. At first sight this is in contradiction with the Drofenik model which attributes the low conductivity for high donor concentrations to the oxidized bulk phase. However Al-Allak *et al.* sintered the holmium-doped samples at 1420 °C [51] and 1460 °C [93], while the sintering temperature during the experiments by Drofenik *et al.* was equal to or lower than 1340 °C. Because of the high sinter temperatures in the experiments conducted by Al-Allak *et al.*, it is possible that the dopant was incorporated without recrystallization and that a reduced form was obtained by equilibration at high temperature. Moreover there are some indications for normal grain growth during sintering at 1420 and 1460 °C. The grain size of the highly doped samples (> 0.3 at %) sintered at 1420 °C [51] is smaller than that of the samples sintered at 1460 °C [93], which is typical for normal grain growth. If the microstructure had been determined by recrystallization, a higher sintering temperature should have resulted in a smaller grain size, as explained previously. This is actually the case for the samples with a donor concentration smaller than 0.3 at %. That suggests that the grain-growth mechanism for low and high donor concentrations is different. Also, the discrepancy between the Drofenik model and the results obtained by Al-Allak *et al.*

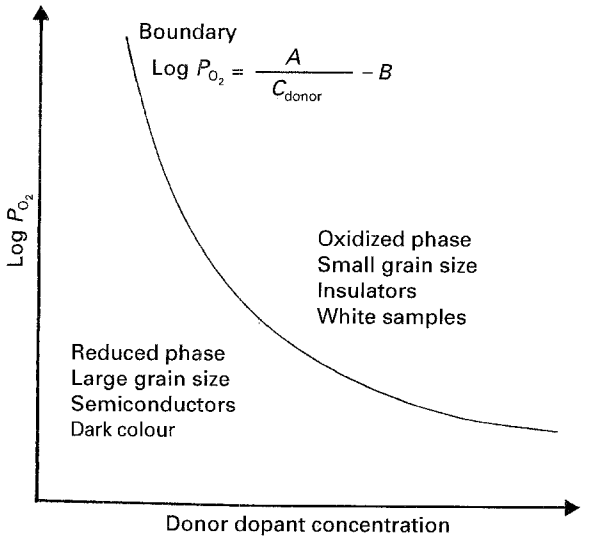

Figure 9 Critical donor dopant levels as a function of the oxygen partial pressure for antimony doping. (——) The boundary line calculated by the thermodynamic model proposed by Drofenik [90].

might be caused by the fact that a different mechanism is making the $BaTiO_3$ semiconductive.

Recently, Desu and Payne [94] explained the anomaly of grain size and conductivity as follows. At low donor concentrations the donors are compensated electronically, giving a high conductivity. When the donor concentration increases the donor concentration at the grain boundary increases even faster, due to segregation. This leads to a vacancy compensation of the donors in the grain-boundary region, resulting in highly resistive grain boundaries. The decrease in grain size was explained by dopant drag on the grain boundaries. As explained above, the grain growth in $BaTiO_3$ occurs by dissolution in a liquid phase and reprecipitation. Therefore, it is not clear how segregation can influence the grain size after sintering. The explanation of Desu *et al.* is in contradiction with the explanation given by Drofenik, who states that in the mixed oxide process the dopant is incorporated during the recrystallization. Also Desu and Payne cannot explain the oxygen release, proportional to the dopant concentration, during grain growth. The proposed model might be valid at high sintering temperature and high donor concentration., when recrystallization does not take place.

Even when the dopant concentration is lower than the critical donor concentration and the material is semiconductive, the charge carrier concentration does not equal the nominal donor concentration in the starting powder. The nominal donor concentration can be 10–20 times higher than the charge carrier density derived from impedance analysis. This phenomenon can be caused by four different mechanisms, which can occur simultaneously: first, partial dissolution of the donor in the liquid phase [95], second, the incorporated donor atoms are partly compensated by acceptor dopants such as manganese or magnesium [30, 84]; third, the incorporated donor atoms are partly compensated by cation vacancies V''_{Ba} or V''''_{Ti}. Several researchers [43, 52, 56, 57] assumed that V''_{Ba} are the compensating defects; however, based on calculations using energy minimization techniques, Lewis *et al.* claim that titanium vacancies are the predominant compensating defect [54, 96]. Also phase studies at higher donor concentrations are consistent with titanium vacancy compensation [55, 97]. Fourth, some donors can be incorporated at equivalent lattice sites but with a different valency, e.g. equal number of Sb^{3+} and Sb^{5+} are incorporated at Ti^{4+} places. This mechanism is called self-compensation [98].

4.2. Oxidation N_s and E_s

At first it should be pointed out that annealing and cooling in an oxidative atmosphere are similar processes which lead to the oxidation of grain boundaries while the inside of the grains is not oxidized [31, 32, 49, 50, 52, 61]. The grain boundary oxidation leads to higher electron-trap densities [32, 49, 50] either by the formation of V''_{Ba}, 3d-elements with higher oxidation states, or by the adsorption of oxygen. Higher electron density leads to a significant change in the PTCR effect, as explained before.

The oxidation rate of non-acceptor-doped semiconductive $BaTiO_3$ is much slower than for acceptor-doped semiconductive $BaTiO_3$ [61]. In non-acceptor-doped PTCR ceramics the oxidation is believed to be due to inward diffusion of V''_{Ba}, while in acceptor-doped PTCR ceramics the oxidation is due to outward diffusion of $V_O^{\cdot\cdot}$ to the grain boundaries. This explains why high P_{O_2} annealing under an oxygen partial pressure of 10 MPa (P_{tot} = 100 MPa) at 1200 °C of non-acceptor-doped $BaTiO_3$ only leads to a small change in the PTCR properties [39], while the same annealing of acceptor-doped semiconducting $Ba_{0.8}Sr_{0.2}TiO_3$ improves the properties significantly [81, 100].

It was found by many authors that for the same oxidation time (cooling time), higher doping concentrations of the appropriate 3d-elements increase N_s [49, 83]. Therefore, the oxidation rate must also increase with increasing acceptor doping. This can be understood by the fact that increasing 3d-elements concentration at the grain boundary increases the $V_O^{\cdot\cdot}$ concentration around the grain boundary. Higher $V_O^{\cdot\cdot}$ concentrations lead to a higher V'_O flux, thereby leaving behind more 3d-elements with a higher oxidation state, acting as electron traps.

One could conclude that it is best to oxidize very thoroughly or to add a sufficient amount of the appropriate 3d-elements as ρ_{max} increases with increasing N_s, and a large resistivity jump is desired for many applications. However, there is a limitation. Because ρ_{min} depends on the spontaneous polarization which is a material constant, there exists a maximum N_s which can be compensated [42, 101]. Above this concentration, ρ_{min} increases very quickly by increasing N_s [42, 59, 93]. Therefore, improvements in PTCR characteristics by increasing N_s are limited.

As explained before, manganese was found to be the most effective additive because it creates deeper traps than V''_{Ba}, adsorbed oxygen and other 3d-elements, thereby generating improved PTCR properties. This seems to lead us now to the fact that significant further improvement by changing the material composition is difficult. However, recently it was found that deeper electron traps can be obtained by annealing under a high P_{O_2} [102, 103]. These traps are believed to be caused by Mn^{4+}. This finding opens new possibilities as previously tested 3d-elements such as chromium, cobalt, iron, etc., might have a 4^+ oxidation state with even deeper traps than Mn^{4+}.

As segregation changes the acceptor concentration near the grain boundary, this should influence the PTCR properties. Segregation in $BaTiO_3$ has been shown to take place by Knauer [104]. Recent work by Chiang *et al.* [67, 105] and Desu *et al.* [94, 106, 107] concerning segregation will prove to be very useful for the understanding of the relation between the PTCR properties and the processing, although discussion still continues about the exact segregation mechanism [108, 109].

5. Conclusion

The Heywang model, which postulated that a two-dimensional layer of electron traps at the grain

boundary creates a Schottky barrier, is generally accepted to model the resistivity–temperature behaviour of semiconductive $BaTiO_3$. It has been shown that the electron traps can be caused by adsorbed oxygen, barium vacancies and or 3d-elements. However, the relation between the processing parameters and the PTCR effect is not yet completely understood.

Phenomena such as segregation, grain growth, grain-boundary oxidation, depend on the processing parameters and influence the electrical properties and therefore the final PTCR. Moreover these phenomena are interrelated in a complex manner. For example, changing the sintering temperature influences segregation, equilibrium defect structure and the oxidation during cooling. The segregation of acceptors can also influence the oxidation rate.

Therefore, only a scientific and multi-disciplinary approach will help us to understand and improve PTCR properties further.

Acknowledgements

The authors thank R. Elst and D. Scholten, Philips Industrial Components, and M. Yodogawa, TDK, who generously provided the photographs.

References

1. PROTEUS, commercial brochure on "Shape-memory alloys". Proteus, Stasegemsestwg 110E-B 8500 Kortrijk, Belgium (Kyodokumiai Insatsu, Nagaoka).
2. R. SHROUT, D. MOFFATT and W. HUEBNER, *J. Mater. Sci.* **26** (1991) 145.
3. L. L. ROHLFING, R. E. NEWNHAM, S. M. PILGRIM and J. RUNT, *J. Wave-Mater. Interact.* **3** (1988) 273.
4. E. KATO and M. HASEGAWA, *J. Chem. Soc. Jpn Ind. Chem. Sect.* **70** [3] (1967) 252.
5. T. OTA, I. YAMAI and I. TAKAHASHI, in "29th Ceramics Basics Science Symposium". Nagaoka, Japan, 24–25 January 1991, 1A08 (1991) p. 8.
6. *Idem, J. Am. Ceram. Soc.* **75** (1992) 1772.
7. R. S. PERKINS, A. RUEGG, M. FISCHER, P. STREIT and A. MENTH, *IEEE Trans. Compon. Hybr. Manuf. Technol.* **5** (1982) 225.
8. B. C. HENDRIX, X. WANG, W. CHEN and W. Q. CUI, *J. Mater. Sci. Mater. Electron.* **3** (1992) 113.
9. M. YETHIRAJ, *J. Solid State Chem.* **88** (1990) 53.
10. B. M. KULWICKI, in "Advances in Ceramics", Vol. 1 "Grain boundary phenomena in electronic ceramics", edited by L. M. Levinson and D. C. Hill (American Ceramic Society, Colombus, OH, 1981) pp. 138–53.
11. B. JAFFE, W. R. COOK and H. JAFFE, in "Piezoelectric Ceramics", edited by J. P. Roberts and P. Popper (Academic Press, London, New York, 1971).
12. Electronic materials manufacturers association of Japan, Constant temperature PTC-heaterguide" (1990).
13. M. KUWABARA and K. KUMAMOTO, *J. Amer. Ceram. Soc.* **66** (1983) 214.
14. L. MEIDONG, I. J. LI, L. HSIWEI, C. ZHIXIONG and Y. XI, *Jpn J. Appl. Phys.* **24** (1985) 308.
15. D. Y. WANG, F. S. HWANG and T. Y. TSENG., *J. Am. Ceram. Soc.* **73** (1990) 2767.
16. T. Y. TSENG and S. H. WANG., *Mater. lett.* **9** (1990) 164.
17. H. NAGOMOTO, H. KAGOTANI and T. OKUBO., *J. Am. Ceram. Soc.* **76** (1993) 2053.
18. Philips Components Industrial, Evere, Brussels (1992).
19. B. M. KULWICKI, PTC materials technology, "Advances in Ceramics", Vol. 1, "Grain boundary phenomena in electronic ceramics, edited by L. M. Levinson and D. C. Hill (American Ceramic Society, Colombus, OH, 1981) pp. 155–66.
20. W. HEYWANG, *Solid State Electron.* **3** (1961) 51.
21. *Idem, J. Am. Ceram. Soc.* **47** (1964) 484.
22. G. H. JONKER, *Solid State Electron* **7** (1964) 895.
23. A. AMIN, *J. Am. Ceram. Soc.* **72** (1989) 369.
24. D. Y. WANG and K. UMEYA, *ibid.* **73** (1990) 669.
25. G. GOODMAN, *ibid.* **46** (1963) 48.
26. H. NEMOTO and I. ODA, *ibid.* **63** (1980) 398.
27. H. SUMINO. O. SAKURAI, K. SHINOZAKI and N. MIZUTANI, *J. Ceram. Soc. Jpn* **100** (1992) 97.
28. H. S. MAITI and R. N. BASU, *Mater. Res. Bull.* **21** (1986) 1107.
29 J. ILLINGSWORTH, H. M. AL-ALLAK, A. W. BRINKMAN and J. WOODS, *J. Appl. Phys.* **67** (1990) 2088.
30 C. J. PENG and H. Y. LU, *J. Am. Ceram Soc.* **71** [1] (1988) C44–46.
31. H. P. CHEN and T. Y. TSENG, *J. Mater. Sci. Lett.* **8** (1989) 1483.
32. A. B. ALLES, V. R. W. AMARAKOON and V. L. BURDICK, *J. Am. Ceram. Soc.* **72** (1989) 148.
33. D. C. SINCLAIR and A. R. WEST, *J. Appl. Phys.* **66** (1989) 3850.
34. M. KUWABARA, *Solid State Electron* **27** (1984) 929.
35. B. ALLES ALDO and V. L. BURDICK, *J. Am. Ceram. Soc.* **76** (1993) 401.
36. S. HISHITA, P. BLANCHART, J. F. BAUMARD and P. ABELARD, *Jap. J. Appl. Phys. Ser.* 2 *Lattice Defects Ceram.* (1989) 167.
37. S. HISHITA, J. F. BAUMARD and P. ABELARD, *Coll. Phys.* **C1** Suppl. 1, **51**, (1990) 979.
38. S. HISHITA, K. ITO, J. F. BAUMARD and P. ABELARD, *J. Ceram. Soc. Jpn Int. Ed.* **98** (8) (1990) 152.
39. S. HISHITA, K. ITO, J.-F. BAUMARD and P. ABELARD, *J. Ceram. Soc. Jpn.* **98** (1990) 885.
40. H. IHRIG and W. PUSCHERT, *J. Appl. Phys.* **48** (1977) 3081.
41. HAANSTRA and H. IHRIG, *J. Am. Ceram. Soc.* **63** (1980) 288.
42. B. HUYBRECHTS, K. ISHIZAKI and M. TAKATA, *ibid.* **75** (1992) 722.
43. J. DANIELS, K. H. HARDTL and R. WERNICKE, *Philips Tech. Rev.* **38**(3) (1978) 73.
44. G. H. JONKER, *Mater. Res. Bull.* **2** (1967) 401.
45. J. DANIELS and R. WERNICKE, *Philips Res. Repts.* **31** (1976) 544.
46. H. IGARASHI, S. HAYAKAWA and K. OKAZAKI, *Jpn. J. Appl. Phys.* **20**(4) (1981) 135.
47. T. TAKAHASHI, Y. NAKANO and N. ICHINOSE, *J. Ceram. Soc. Jpn.* **98** (1990) 879.
48. WERNICKE R., *Philips Res. Repts* **31** (1976) 526.
49. H. M. AL-ALLAK, G. J. RUSSEL and J. WOODS, *J. Phys. D Appl. Phys.* **20** (1987) 1645.
50. TSAI-FA LIN, CHEN-TI HU and I-NAN LIN, *J. Mater. Sci.* **25** (1990) 3029.
51. H. M. AL-ALLAK, A. W. BRINKMAN, G. J. RUSSEL A. W. ROBERTS and J. WOODS, *J. Phys. D Appl. Phys.* **21** (1988) 1226.
52. HONG-SOO KIM, GUN YONG SUNG and CHONG HEE KIM, *J. Am. Ceram. Soc.* **75** (1992) 587.
53. G. V. LEWIS, C. R. A. CATLOW and R. E. W. CASSELTON, *ibid.* **68** (1985) 555.
54. G. V. LEWIS and C. R. A. CATLOW, *Br. Ceram. Proc.* **36** (1985) 187.
55. M. H. CHAN, M. P. HARMER and D. M. SMYTH *J. Am. Ceram. Soc.* **69** (1986) 507.
56. G. KOSCHEK and E. KUBALEK, *ibid.* **68** (1985) 582.
57. G. KOSCHEK, *DKG* **66**(3/4) (1989) 128.
58. H. IHRIG, *J. Am. Ceram. Soc.* **64** (1981) 617.
59. H. UEOKA and M. YODOGAWA, *IEEE Trans. Manuf. Technol.* **3**(2) (1974) 77.
60. H. UEOKA, *Ferroelectrics* **7** (1974) 351.
61. H. M. AL-ALLAK, A. W. BRINKMAN, G. J. RUSSEL and J. WOODS, *J. Appl. Phys.* **63** (1988) 4530.
62. H. J. HAGEMANN and H. IHRIG, *Phys. Rev. B* **20** (1979) 3871.

63. H. J. HAGEMANN and D. HENNINGS, *J. Am. Ceram. Soc.* **64** (1981) 590.
64. T. R. N. KUTTY and P. MURUGARAJ, *Mater. Lett.* **3** (5,6) (1985) 195.
65. T. R. N. KUTTY, P. MURUGARAJ and GAJBHIYE, *Ibid.* **2** (5A) (1984) 396.
66. T. R. N. KUTTY, D. L. GOMATHI and P. MURUGARAJ, *Mater. Res. Bull.* **21** (1986) 1093.
67. Y. M. CHIANG and T. TAKAGI, *J. Am. Ceram. Soc.* **73** (1990) 3286.
68. S. B. DESU and D. A. PAYNE, *ibid.* **73** (1990) 3416.
69. Y. MATSUO, M. FUJIMURA, H. SASAKI, K. NAGASE and S. HAYAKAWA, *Ceram. Bull.* **47** (1968) 292.
70. H. F. CHENG, *J. Appl. Phys.* **66** (1989) 1382.
71. V. RAVI and T. R. N. KUTTY, *J. Am. Ceram. Soc.* **75** (1992) 203.
72. H. M. O'BRYAN and J. THOMSON, *ibid.* **57** (1974) 522.
73. K. W. KIRBY and B. A. WECHSLER, *ibid.* **74** (1991) 1841.
74. D. E. RASE and ROY RUSTUM, *ibid.* **38** (1955) 389.
75. Y. MATSUO and H. SASAKI, *ibid.* **54** (1971) 471.
76. D. F. K. HENNINGS, R. JANSSEN and P. J. L. REYNEN, *ibid.* **70** (1987) 23.
77. TSAI-FA LIN, CHEN-TI HU and I-NAN LIN, *ibid.* **73** (1990) 531.
78. H. M. AL-ALLAK, T. V. PARRY, G. J. RUSSEL and J. WOODS, *J. Mater. Sci.* **23** (1988) 1083.
79. D. HENNINGS, *Sci. Ceram.* **12** (1984) 405.
80. S. OSAKI, B. HUYBRECHTS and K. ISHIZAKI, *J. Ceram. Soc.* **101** (1993) 955.
81. B. HUYBRECHTS, *J. Eur. Ceram. Soc.* **11** (1993) 395.
82. IN-CHYUAN HO and SHEN-LI FU, *J. Am. Ceram. Soc.* **75** (1992) 728.
83. H. SCHMELZ and A. MEYER, *DKG* **59** (1982) 436.
84. C. J. TING, C. J. PENG, H. Y. LU and S. T. WU, *ibid.* **73** (1990) 329.
85. S. SHIRASKI and K. KAKEGAWA in "Fine Ceramics", edited by S. Saito (Elsevier Science, New York, 1985) pp. 150–61.
86. A. HASEGAWA, FUJITSU SATORU, K. KOUMOTO and H. YANAGIDA, *J. Ceram. Soc. Jpn* **99** (1991) 718.
87. G. H. JONKER and E. E. HAVINGA, *Mater. Res. Bull.* **17** (1982) 345.
88. M. DROFENIK, A. POPOVIC, L. IRMANCNIK, D. KOLAR and V. KRASEVEC, *J. Am. Ceram. Soc.* (1982) C203.
89. M., DROFENIK, A. POPOVIC and D. KOLAR, *Ceram. Bull.* **63** (1984) 702.
90. M. DROFENIK, *J. Am. Ceram. Soc.* **70** (1987) 311.
91. *Idem, ibid.* **73** (1990) 1587.
92. *Idem, ibid.* **69** (1986) C8.
93. H. M. AL-ALLAK, J. ILLINGSWORTH, A. W. BRINKMAN, G. J. RUSSEL and J. WOODS. *J. Appl. Phys.* **64** (1988) 6477.
94. S. B. DESU and D. A. PAYNE, *J. Am. Ceram. Soc* **73** (1990) 3407.
95. P. BLANCHART, J. F. BAUMARD and P. ABELARD, *ibid.* **75** (1992) 1068.
96. G. V. LEWIS and C. R. A. CATLOW, *Rad. Effects* **73** (1983) 307.
97. G. H. JONKER and E. E. HAVINGA, *Mater. Res. Bull.* **17** (1982) 345.
98. W. HEYWANG, *J. Mater. Sci.* **6** (1971) 1214.
99. B. HUYBRECHTS, K. ISHIZAKI and M. TAKATA, in "Gas Pressure Effects on Materials Processing and Design", edited by K. Ishizaki, E. Hodge, M. Concannon, Vol. 251 (MRS. Pittsburg, PA, 1992) pp. 239–44.
100. B. HUYBRECHTS, K. ISHIZAKI and M. TAKATA, in "Grain Boundary Controlled Properties of Fine Ceramics, edited by K. Ishizaki, K. Niihara, M. Isotani, and R. Ford (Elsevier Science, London, 1992) pp. 32–9.
101. G. H. JONKER, in "Advance in Ceramics", Vol. 1, "Grain boundary phenomena in electronic ceramics", edited by L. M. Levinson and D. C. Hill (American Ceramic Society, Colombus, OH, 1981) pp. 155–66.
102. B. HUYBRECHTS, K. ISHIZAKI and M. TAKATA, *J. Am. Ceram. Soc.* **77** (1994) 286.
103. *Idem*, in "Hot Isostatic Pressing '93", edited by L. Delaey, W. Tas and W. Kaysser (Elsevier Science, Amsterdam, 1993) pp. 451–8.
104. U. KNAUER, *Phys. Status Solidi* **53** (1979) 207.
105. Y. M. CHIANG and T. TAKAGI *J. Am. Ceram. Soc.* **73** (1990) 3278.
106. S. D. DESU and D. A. PAYNE, *ibid.* **73** (1990) 3398.
107. *Idem, ibid.* **73** (1990) 3391.
108. Y. M. CHIANG and T. TAKAGI, *ibid.* **75** (1992) 2017.
109. S. B. DESU and D. A. PAYNE, *ibid.* **75** (1992) 2020.

Received 2 May
and accepted 19 August 1994